

Finite element analyses of Wanjiashai water transmission tunnel excavation and service

Wang Xiequn¹ Wang Zhao² Huang Jie² Wang Junqi²

(¹College of Civil Engineering and Architecture, Wuhan University of Technology, Wuhan 430070, China)

(²School of Civil Engineering, Wuhan University, Wuhan 430072, China)

Abstract: This paper is devoted to the nonlinear stress and strain analysis of tunneling and working conditions of Wanjiashai Division Project No.7 Tunnel in Shanxi province of China. The initial geological stress of loess was simulated by grading fill; the theory of unloading proposed by Duncan and boundary stress of elasticity were used to calculate the excavation of the tunnel; Goodman joint elements were applied to simulate the joints of the liners; both loading and unloading tests have been performed to determine the parameters of Duncan-Chang's model and the calculated results were compared; Terzaghi's theory on loosening earth pressure was applied. Many working conditions were analyzed and some reasonable results were obtained. Based on the analyses, reparative measures were proposed and completed. The tunnel has functioned well since October, 2001.

Key words: tunnel; loess; nonlinear finite element method; loading and unloading test; loosening earth pressure; stress; strain

The Wanjiashai reservoir on the Yellow River located in northwest of Shanxi province in China has a capacity of 8.96 Gm³ and the Wanjiashai Yellow River Division Project, which transmits a discharge of 48 m³/s to Taiyuan city (capital of Shanxi province) mainly consists of nonpressure tunnels of more than 210 km. The No.7 tunnel located between the Gejia Mountain and the Shuiquan river of Pianguan county is 9.21 km long and in its total length, the part of earth tunnel about 2.685 km long has a tunneling diameter of 6.012 m, internal diameter of 5.46 m and precast concrete liner thickness of 0.25 m. Every ring of liner is composed of 4 hexagon segments. The space between tunnel wall and segments is backfilled with grouted pea gravel. Some parts of No.7 tunnel pass through loess of geological age Q_3 . Because of applying tunnel boring machine (TBM) in these loess parts, which is usually used in rock tunneling, there emerged sinking, over excavation and loose filling phenomena in the soil mass. So the segments, between CH 0 + 941 and CH 1 + 322, were dislocated, the maximum distance of dislocation was nearly 100 mm, meanwhile the fissures, of which the maximum width was about 1 mm, emerged in 204 segments. To analyze the stress and deformation of the tunnel wall and segment under the pressure of surrounding soil and also when it is in

service or in depletion of water, the finite element method (FEM) was performed in No.7 earth tunnel.

1 Finite Element Mesh Used in Simulation

The analysis of stress and deformation of the long tunnel was a plane strain problem and Fig.1 indicates mesh of FEM of transect 0 + 63 of tunnel No.7. In Fig. 1, the bottom nodes are fixed hinge bearings, and the left and right nodes are horizontal link bearings. The quadrangle meshes firstly were made manually, then formed triangle meshes automatically while the soil element formed a quadrangle. The soil elements in tunneling section were replaced by air elements during tunneling; and the concrete segment liner was divided into three rings of quadrangle elements of 6 cm, 13 cm and 6 cm in radius direction, respectively. There are 3 Goodman joint elements in the joint of every two segments. So there are 12 Goodman joint elements in 4 joints of 4 segments. Each thickness of the two rings of the quadrangle elements in the grouted pea gravel is 5 cm (see Fig.2).

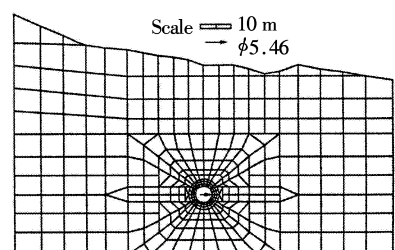


Fig.1 FEM mesh of cross section 0 + 63 in tunnel No.7

Received 2003-06-23.

Biographies: Wang Xiequn (1971—), female, graduate, lecturer, xq001wang@hotmail.com; Wang Zhao (corresponding author), male, doctor, professor, wazh@public.wh.hb.cn.

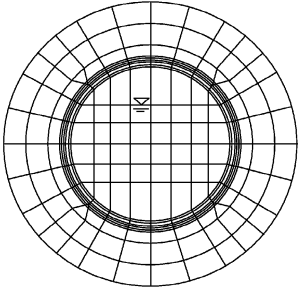


Fig.2 Mesh of tunnel liner

2 Constitutive Model and Parameters of Calculation

Duncan-Chang’s nonlinear E - μ model, and his loading-unloading principle, which was modified in 1984^[1], were employed. Where E is the tangent modulus; μ is the Poisson’s ratio; k, n, R_f, G, F, D are parameters of the model; c is the cohesion and φ is the angle of internal friction.

Based on Mohr-Coulumb failure criterion of soil, when the stress circle of element intersects the failure envelope, keeps σ_y unchanging, decreases the radius of the stress circle until it is tangential to the failure envelope and calculate the σ_x, τ_{xy} as element stress, furthermore transfers the surplus stress into nodal loads.

Using linear elasticity model^[2] in the concrete liner and pea gravel layer, when σ_1 is beyond compre-

ssive strength or σ_3 is less than tensile strength, the element failed and the surplus stress didn’t transfer. σ_1 and σ_3 are major and minor principle stresses.

Practically, tunneling is an unloading process, but the parameters of Duncan-Chang’s model are obtained from the conventional triaxial test, which is a loading test. So parameters obtained from the unloading test are needed to simulate the stress path of the soil elements in the unloading state. Moreover, the results from the unloading test must be compared with the results from the loading test with respect to the principle of loading and unloading (see Tab.1).

Tab.1 A comparison between E and μ from loading and unloading tests

Tests	Parameters	σ_3/kPa		
		300	500	700
Loading	E/GPa	63.0	69.4	79.3
	μ	0.35	0.31	0.27
Unloading	E/GPa	67.4	126	180
	μ	0.431	0.433	0.436

In Tab.2, parameters of saturated soil are used in soil elements that are submerged because of seepage; and parameters of loosening soil are used in soil elements within the 2 m circle realm beyond the tunnel. Module parameters of concrete segments, joints of segments and layers of grouted pea gravel, determined by relative tests, are listed respectively in Tab.3 and Tab.4.

Tab.2 Model parameters and mechanical properties of nonlinear materials

	Nonlinear material	$\gamma/(\text{kN} \cdot \text{m}^{-3})$	c/kPa	$\varphi/(^{\circ})$	k	n	R_f	G	F	D
Loading test	Natural soil	17.8	0	30.1	426	0.19	0.89	0.45	0.21	5.0
	Saturated soil	19.1	20	20.2	246	0.43	0.88	0.33	0.09	3.0
	Loosening soil	16.1	21	18.5	288	0.26	0.88	0.49	0.22	4.2
Unloading test	Natural soil	17.8	5	38.0	216	1.13	0.99	0.42	- 0.02	0.04

Tab.3 Model parameters and mechanical properties of linear materials

Linear material	$\gamma/(\text{kN} \cdot \text{m}^{-3})$	E/GPa	μ	f_{cm}/MPa	f_t/MPa
Concrete segment	25.0	30.0	0.167	16.5	1.50
Grouted pea gravel	23.0	22.0	0.167	8.5	0.90
Grouted pea gravel	20.5	14.5	0.130	4.1	0.55

Note: f_{cm} is the compressive strength; f_t is the tensile strength; γ is the moist unit weight.

Tab.4 Model parameters and mechanical properties of joints

Joints	$\varphi_s/(^{\circ})$	c_s/kPa	R_{fs}	k_s	n_s
Soil to soil	30.1	10	0.88	10^4	0.51
Segment to segment	34.0	100	0.75	10^4	0.65

3 Calculation Scheme and Simulation of Construction Process

3.1 Calculation scheme

The calculation scheme was performed as follows:
① Simulation of initial stress forming^[3] in the process

of filling soil mass; ② Simulation of stress relief and displacement distribution of the tunnel wall arising from excavation; ③ Determination of stress and deformation of segments and pea gravel arising from self-gravity and the effect of the surrounding loosening soil; ④ Determination of displacement and stress of segments under the condition of service and depletion of water.

3.2 The method of load relief in tunneling

The concept of load relief was put forward by

Duncan^[1]. To apply this method, the stages were as follows; firstly, the external boundary was assumed to be broad enough, for example, three or four times broader than the tunneling diameter; then, the initial stress field before excavation of the tunnel was calculated, $\sigma_0 = [\sigma_x, \sigma_y, \tau_{xy}]_0^T$; and the plane force x, y in the tunneling boundary was calculated^[4] too, where α was the angle between external normal direction of the boundary and X axle.

$$\begin{cases} X = \sigma_x \cos \alpha + \tau_{xy} \sin \alpha \\ Y = \sigma_y \sin \alpha + \tau_{xy} \cos \alpha \end{cases} \quad (1)$$

Then, according to plane force, the equivalent nodal force was calculated, then exerted on tunnel wall as load and the increment of the stress $\Delta\sigma$ and the increment of displacement δ were calculated too. Finally, the stress field after excavation of the tunnel was equal to the sum of the initial stress and increment of stress, which was $\sigma = \sigma_0 + \Delta\sigma$, where δ arising from excavation of the tunnel was just the deformation of the tunnel wall and surrounding soil.

3.3 Loosening earth pressure

Due to the arching effect of the soil in the tunnel crown, the pressure on the segment wasn't equal to the self-gravity of the upper cover soil but depended on the pressure of the upper loosening soil after the liner was installed. Test and theoretical deduction have been done by Terzaghi (1936) to determine the realm of loosening soil. The height of loose soil from horizontal diameter to the above was three times that of the diameter^[5]. Assuming the coefficient of static soil pressure to be $k_0 = 1 - \sin \varphi$, the external pressure on the liner could be taken as nodal force to calculate the stress and deformation of segments.

3.4 Simulation program of construction process

In finite element analysis, the accumulation of soil mass was simulated by exerting increments of self-gravity layer by layer and the initial stress within the soil mass was also calculated; the variation of water level was simulated by varying of water pressure on internal side of the segment. The load was graded into fifteen levels according to the mesh in 0 + 63 transect of No.7 tunnel. The soil elements were set in layers of the liner and pea gravel before excavation of tunnel during simulation, and the parameters of Goodman elements were the parameters of soil to soil (see Tab.4). After tunneling, the excavation element was set by air element and corresponding changes of parameters were

made in liner, pea gravel and Goodman elements to make calculation convenient.

In the finite element analysis of simulating the accumulation of soil mass, the calculated stress of new elements in each grade is added to total stress of elements, but the nodal displacement was ignored. The increment of water pressure due to variation of water level was exerted directly on corresponding nodes of the segment. The submerged unit weight of the soil elements in the scope of water descending was substituted by saturated unit weight, while in the realm of water ascending, wet unit weight was substituted by submerged unit weight. And the variation of self-gravity of soil elements in the scope of water was changed into nodal forces.

4 Results of Finite Element Analyses

There are mainly three parts of the results of the calculation; firstly, the displacement and stress distribution of the calculation profile; secondly, nodal displacement vectors on the internal side of the tunnel wall and segments; thirdly, stress distribution of concrete segments and grouted pea gravel.

4.1 Analysis and comparison of displacement

4.1.1 Nodal displacement of tunnel wall after tunneling

Fig.3(a) and Fig.3(b) indicate the outline of displacements of 8 nodes on tunnel wall after tunneling. Among the eight displacement vectors, numerator stands for horizontal displacement (the positive direction is to the right) and denominator stands for vertical displacement (the positive direction is upward). Apparently, nodal displacement isn't symmetrical and horizontal displacement inclines to the thinner side of upper soil mass. Fig.3(a) indicates the calculated results based on parameters from loading test together with loading-unloading principle; Fig.3(b) indicates the calculated results from unloading test

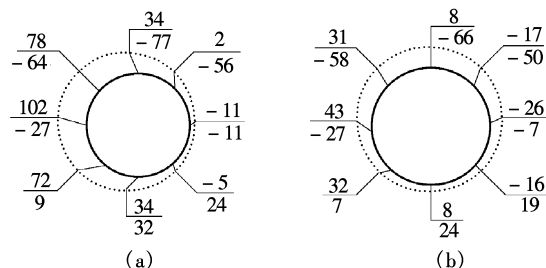


Fig.3 Excavation displacement of section 0 + 63 in tunnel No.7 (mm). (a) Loading test; (b) Unloading test

parameters, which shows that the displacements calculated on unloading test parameters are less. Furthermore, it is reasonable that the horizontal displacements are dissymmetrical caused by slight asymmetry of upper soil mass.

4.1.2 Nodal displacement of internal side of segment

The laws of nodal displacement of internal side of segments are presented and compared as follows.

A considerable increment of displacement occurred at Grade eleven when exerting loosening earth pressure and Grade fourteen when affected by two-sided water pressure on liners when the water level in the tunnel descended to zero with seepage in liner. The displacement of four points, i.e., intersection points of the tunnel wall and coordinates X , Y , and the variation of height and width of the tunnel under Grade eleven is shown in Tab.5 and Grade fourteen is shown in Tab.6.

Tab.5 Comparison of displacement inside of liner (under loosening earth pressure) mm

Parameters	Top		Bottom		Height decrease	Left		Right		Width decrease
	U_X	U_Y	U_X	U_Y		U_X	U_Y	U_X	U_Y	
Loading test	-1	-19	2	-18	1	0	-20	1	-16	1
Unloading test	0	-18	0	-17	1	0	-18	0	-18	0

Tab.6 Comparison of displacement inside of liner (inside empty and outside water pressure) mm

Parameters	Top		Bottom		Height decrease	Left		Right		Width decrease
	U_X	U_Y	U_X	U_Y		U_X	U_Y	U_X	U_Y	
Loading test	-1	-25	1	-24	1	0	-26	1	-23	1
Unloading test	0	-22	0	-21	1	0	-21	0	-22	0

Tab.5 shows that the segments sink integrally about 16 to 20 mm. The relative deformation (for example the variation of the height and the width) is less than 1 mm.

Displacement occurring in Grade fourteen is listed in Tab.6. On the one hand, when the internal water pressure turns to zero, there is a trend that the tube is uplifted due to external water pressure. On the other

hand, the trend is descending, because of the variation of unit weight of the surrounding soil from the submerged unit weight to saturated unit weight. To sum up, the segments sink integrally under the effect of two opposite trends and the sinking increment is less than 6 mm; the relative deformation is less than 1 mm.

4.1.3 Joint dislocation of segments

The greatest joint dislocation of segment is 1 mm in X direction or Y direction under the condition of seepage in normal service.

4.1.4 The displacement field

In tunneling, the isograph of vertical displacement (U_Y) is approximately symmetrical and the axis of symmetry is inclined to the thicker side from the center of the tunnel vertically to the top. The maximal descending of surface is 23 mm, while the surface settlement above the tunnel center is 18 mm.

4.2 Analysis and comparison of stress

1) Concrete segments and layer of grouted pea gravel

The calculated results show that the maximum compressive stress always appeared on the elements of the internal surface of the lateral arch near the horizontal symmetry axis of the tunnel and that the maximum tensile stress often appeared on the internal surface of the top arch or bottom arch near the vertical symmetry axis of the tunnel. Tab.7 gives the principal stress of concrete segments under different loading grades. The design compressive strength of concrete segment is 16.5 MPa and the design tensile strength of concrete segment is 1.5 MPa (see Tab.3). So the elements of the internal surface of the segment won't fail in any working conditions. From Tab.7 the maximum compressive stress and maximum tensile stress of the segment are less than design strength, so the safety coefficients are great. The results of stress

Tab.7 σ_{1max} and σ_{3max} of concrete segment kPa

Section and scheme		Stress and location	Load grade				
			11	12	13	14	15
7# tunnel 0 + 63 (parameters from loading test)	σ_{1max}	Right arch	3 310	3 180	3 320	3 800	3 650
		Left arch	2 430	2 350	2 390	3 880	3 780
	σ_{3max}	Top arch	- 140	- 130	- 180	- 210	- 180
		Bottom arch	- 270	- 310	- 230	- 180	- 110
7# tunnel 0 + 63 (parameters from unloading test)	σ_{1max}	Right arch	2 800	2 780	2 820	3 610	3 490
		Left arch	2 440	2 220	2 430	2 490	2 400
	σ_{3max}	Top arch	- 70	- 70	- 70	- 100	- 100
		Bottom arch	- 50	- 10	- 30	- 70	- 70

calculated from parameters of unloading test are less than those coming from the parameters of the loading test. The results in the layer of grouted pea gravel are the same as those in the concrete segments, not presented here.

2) Stress distribution of transect

The initial stress field arising from the form of the transect, including the isographs of σ_1 and σ_3 , is in accord with the pattern of increasing with the increment of depth. σ_1 and σ_3 are calculated by simulation of the filling process of loess progressively by FEM. The number of failing elements surrounding the tunnel in the realm of 2 m is more than half of the total number.

5 Conclusions

In order to explain the failure phenomena occurring concrete segments and simulate the excavation and working situation of the No. 7 Tunnel of Wanjiazhai Division Project, the finite element method has been used to analyze the stress and strain of the tunnel. The following conclusions can be drawn:

1) It is more reasonable to use parameters from unloading test to calculate the strain and stress of tunnel. The value is less than the results from parameters of loading test together with loading-unloading principle.

2) From analyses of the excavation, under loosening soil pressure, working conditions and depletion, it can be concluded that the stress and strain of segments and surrounding grouted pea gravel are not beyond the allowable values and will not cause

fissure and obvious dislocation in segments. The most serious condition is when seepage occurs in liners during the depletion of water.

3) It is practical to use the unloading theory proposed by Duncan and boundary stress of elasticity for calculation of tunnel excavation, to use Goodman joint element to simulate the liner joint, and to use Terzaghi's theory of loosening earth pressure to exert earth pressure. But the incline of the stratum surface cannot be taken into account by Terzaghi's theory.

Wanjiazhai Division Project has been put into water transmission trial since Oct. 2001 and remains in good condition up till now.

References

- [1] Duncan J M, Seed R B, Wong K S, et al. A computer program for finite element analysis of dams [R]. Geotechnical Engineering Research Report No. SU/GT/84-3. Stanford University, 1984.
- [2] Timoshenko S P, Goodier J N. *Theory of elasticity*. 3rd Ed [M]. New York: McGraw-Hill Book Company, 1970. 291 - 349.
- [3] Lubliner J. *Plasticity theory* [M]. New Jersey: Prentice-Hall, 1998. 280 - 283.
- [4] Xu Zhilun. *Mechanics of elasticity* [M]. Beijing: The People's Educational Press, 1979. 33 - 34. (in Chinese)
- [5] Terzaghi K. Stress distribution in dry and in saturated sand above a yielding trap-door [A]. In: *Proceedings of 1st Conference of Soil Mechanics and Foundation Engineering* [C]. Boston, 1936, 1: 307 - 316.

万家寨引水隧洞成洞和运行的有限元分析

王协群¹ 王 钊² 黄 杰² 王俊奇²

(¹ 武汉理工大学土木工程与建筑学院, 武汉 430070)

(² 武汉大学土木建筑工程学院, 武汉 430072)

摘 要 对山西省万家寨引黄入晋工程总干线 7 号隧洞开挖和蓄水运行的几种工况进行了非线性有限元分析. 主要内容包括采用分级堆填过程模拟风积黄土层的初始应力场; 应用 Duncan 释放荷载思想和弹性理论面力公式进行开挖卸荷计算; 采用 Goodman 节理单元模拟衬砌管片的接缝; 应用 Terzaghi 松动土压力理论施加管片上压力; 确定土的 Duncan-Chang 模型参数时, 分别取原状土进行了卸载和加载试验, 并比较了用 2 种试验获得的模型参数进行有限元变形分析的结果, 多种工况的有限元分析得到了一些合理的结果.

关键词 隧洞; 黄土; 非线性有限元方法; 加卸载实验; 松动土压力; 应力; 应变

中图分类号 TU43